Constraints on Axion-Like Particles from Stellar Evolution with MESA

Kudashov A.M.

Faculty of Physics, Lomonosov Moscow State University
Institute for Nuclear Research of the Russian Academy of Sciences

Quarks-2026

Outline

From Main Sequence to the Red Giant Branch

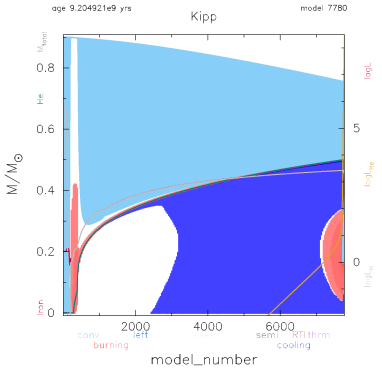

Evolutionary picture

- Central H burning on the MS
- H is exhausted in the center
- An inert He core forms
- H burning continues in a shell
- The star ascends the RGB

Key point

An RGB star consists of a degenerate helium core surrounded by a thin hydrogen-burning shell, embedded in a cool, extended convective envelope.

Evolution on the HR Diagram

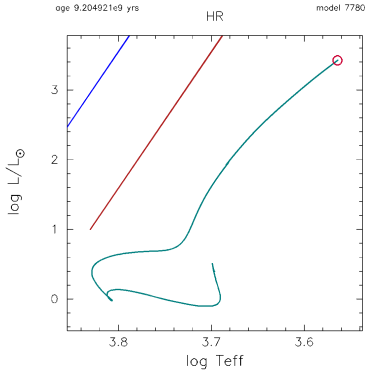

HR-diagram path

- The star leaves the main sequence after central hydrogen exhaustion.
- An inert helium core appears in the center.
- Hydrogen burning continues in a shell around the core.
- The envelope expands and the surface cools.
- The luminosity increases as the star moves up the RGB.

RGB Luminosity and He-Core Mass

Shell-source homology

Analytic approach of Refsdal and Weigert:

$$T_{\rm shell} \sim \frac{M_c}{R_c}$$

$$L \sim M_c^7 R_c^{-16/3}$$

Physical meaning

As the helium core grows, the shell temperature increases. For CNO burning this strongly increases the luminosity.

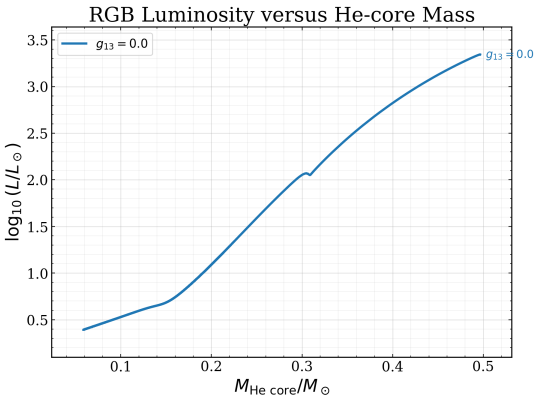

Envelope Expansion on the RGB

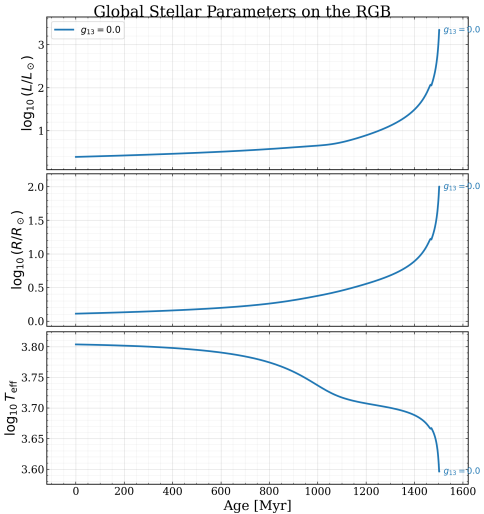

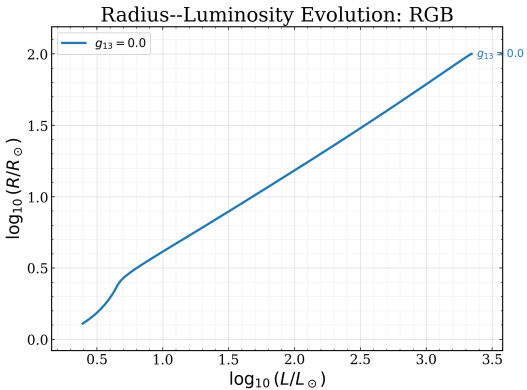

RGB expansion

- The luminosity increases as the H-burning shell becomes stronger

Toward the Tip of the RGB

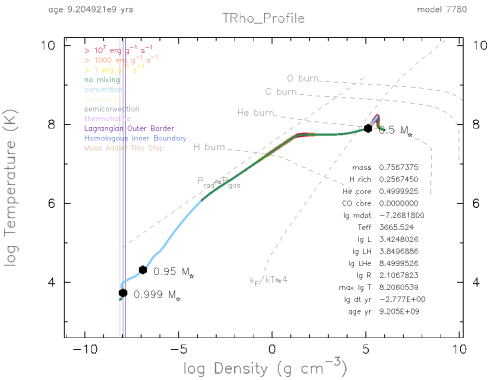

Core heating

- He-core contraction
- Heating by the H-burning shell
- Increasing shell temperature

Helium ignition

- Near TRGB:

$$T \sim 10^8\,\mathrm{K}$$

- Degeneracy is lifted
- Core expands
- Star leaves the RGB

Neutrino Cooling and Off-Center Heating

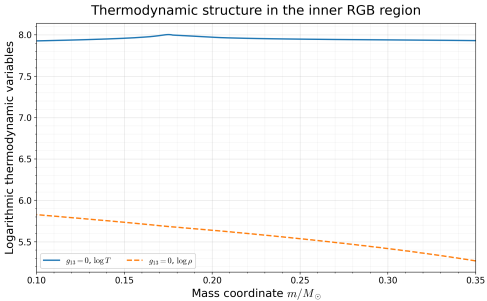

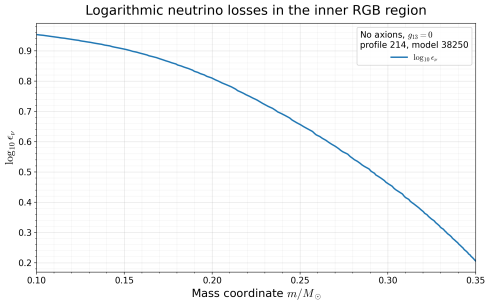

Main point

- Central neutrino cooling shifts the temperature maximum away from the center.
- Therefore, the inner RGB structure is sensitive to additional weakly interacting cooling channels, e.g. axion-like particles.

Axion Implementation in MESA

Bremsstrahlung channel

$$\varepsilon_B^{(\mathrm{nd})} \simeq 47\, g_{ae}^2 T^{2.5} \frac{\rho}{\mu_e} \sum_j \frac{X_j Z_j}{A_j} \left(Z_j + \frac{1}{\sqrt{2}} \right)$$

$$\varepsilon_B^{(\mathrm{d})} \simeq 8.6 \times 10^{-7} F\, g_{ae}^2 T^4 \sum_j \frac{X_j Z_j^2}{A_j}$$

$$\varepsilon_B = \frac{\varepsilon_B^{(\mathrm{d})} \varepsilon_B^{(\mathrm{nd})}}{\varepsilon_B^{(\mathrm{d})} + \varepsilon_B^{(\mathrm{nd})}}$$

Local energy-loss term

$$\varepsilon_a = \varepsilon_B + \varepsilon_C, \qquad g_{13} \equiv \frac{g_{ae}}{10^{-13}}.$$

Compton-like channel

$$\varepsilon_C^{(\mathrm{nd})} \simeq 2.7 \times 10^{-22} g_{ae}^2 \frac{1}{\mu_e} \left(\frac{n_e^{\mathrm{eff}}}{n_e} \right) T^6$$

$$F_{\mathrm{deg}} = \frac{n_e^{\mathrm{eff}}}{n_e} = \frac{3 E_F T}{p_F^2}, \qquad S_{\mathrm{deg}} = \left(1 + F_{\mathrm{deg}}^{-2} \right)^{-1/2}$$

$$\varepsilon_C = \varepsilon_C^{(\mathrm{nd})} S_{\mathrm{deg}}$$

Numerical implementation

The additional losses were added as a local cooling contribution in the MESA `neu` microphysics module. Integrated over the stellar model value.

$$L_a = \int \varepsilon_a \, dm$$

Axion Production Channels in the Inner RGB Region

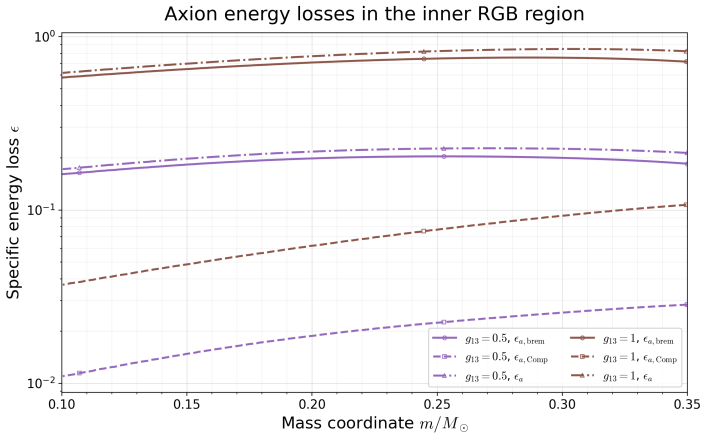

Bremsstrahlung

Bremsstrahlung losses mainly follow the temperature profile. The density dependence is weak, because the correction factor is of order unity.
Therefore the maximum losses occur near the temperature maximum, close to the helium ignition region.

Compton

Compton production is suppressed by Pauli blocking. In the degenerate core, only electrons near the Fermi surface can participate.

Axion Cooling Compared to Neutrino Cooling

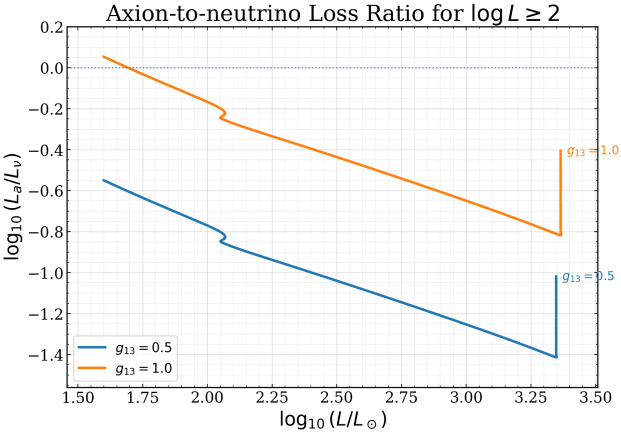

Main point

Before the RGB bump, axion losses are comparable to neutrino losses.

TRGB Luminosities of Real Clusters with MESA

Model setup

- Real globular-cluster parameters: Z, Y, $[\alpha/\mathrm{Fe}]$
- Initial mass chosen from the cluster age
- Evolution from MS to helium ignition
- Output: L_{TRGB}, M_{He}, age at He ignition
- RGB mass loss: Reimers wind

Interior physics

- MESA EOS and nuclear reaction network
- Standard thermal neutrino losses
- Electron conduction included
- Blouin conductive corrections for moderately degenerate plasma
- Element diffusion and gravitational settling included

Opacity and atmosphere

- High-T opacity: OPAL tables
- Mixture: Grevesse & Sauval 1998, α-enhanced
- Low-T opacity: Ferguson et al. tables
- Type 2 opacity for C/O-enhanced regions
- Atmosphere: grey Eddington T–τ relation

Mixing

- Ledoux criterion
- MLT convection, Cox formulation
- $\alpha_{\mathrm{MLT}} = 1.82$
- Semiconvection: Langer prescription
- $\alpha_{\mathrm{sc}} = 0.01$

Main references

MESA: Paxton et al. 2011, 2013, 2015, 2018, 2019; Jermyn et al. 2023. Opacity: Iglesias & Rogers 1996; Ferguson et al. 2005; Grevesse & Sauval 1998. Conductivity: Cassisi et al. 2007; Blouin et al. 2020. Neutrinos: Itoh et al. 1996. Nuclear rates: Angulo et al. 1999; Cyburt et al. 2010. Diffusion: Thoul et al. 1994; Iben & MacDonald 1985. Convection and mass loss: Cox & Giuli 1968; Langer 1985; Reimers 1975.

Globular Cluster Model and Axion Grids

Cluster Model

Our group obtained stellar-population parameters for 27 globular clusters. Each cluster was modeled with MESA up to the TRGB.

Clusters

NGC6205, NGC6218, NGC6093, NGC0288, NGC6171, NGC6352, NGC6838, NGC7099, NGC6723, NGC6362, NGC5897, NGC6366, NGC5024, NGC5272, NGC5904, NGC6341, NGC0362, NGC5053, NGC5466, NGC6779, NGC6101, NGC1261.

Axion-loss grid

For each cluster we computed a grid in g_{13} and will use it to constrain the axion–electron interaction.

g_{13}	$\log L_{\rm TRGB}$	$M_{\rm He,TRGB}$
0.0	3.373	0.4916
0.1	3.373	0.4916
0.2	3.374	0.4918
0.3	3.375	0.4920
0.4	3.376	0.4922
0.5	3.378	0.4927
1.0	3.392	0.4957

Example: NGC0288

TRGB Luminosity and Helium-Core Mass: NGC6063

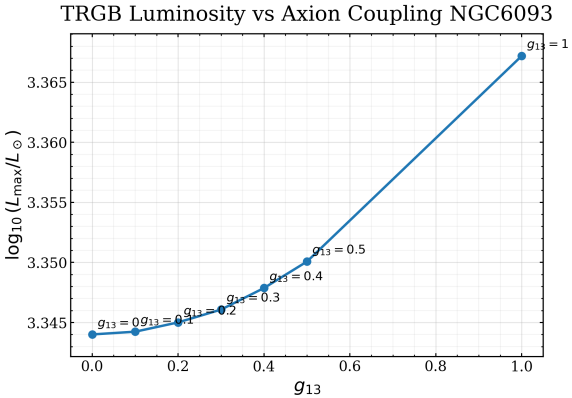

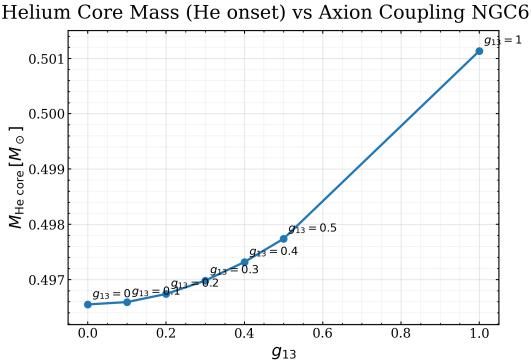

TRGB luminosity

Increasing g_{13} makes the TRGB brighter.

Helium-core mass

Axion cooling delays helium ignition, allowing the He core to grow.

Evolutionary Age Shift: NGC6093

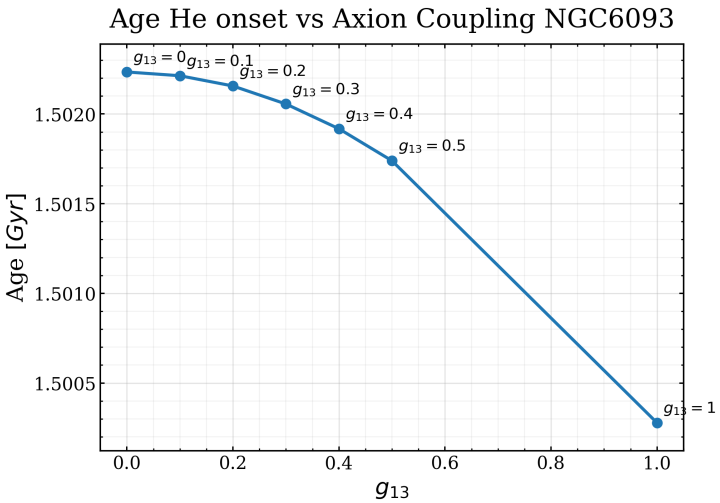

Age at the RGB tip

- The age changes only weakly compared with the luminosity and core mass
- The dominant observable effect is the shift of the TRGB luminosity
- The result is more naturally interpreted through the He-core mass

Hot-Flasher Transition Regime: NGC6366

Axion grid for NGC6366

g_{13}	$\log L_{\max}$	$M_{\mathrm{He,TRGB}}$
0.1	3.406	0.483
0.2	3.406	0.483
0.3	3.406	0.483
0.4	3.406	0.483
0.5	3.407	0.483
1.0	3.409	0.483

Mass loss

NGC6366 has the largest Reimers mass loss in the sample:

$$\eta = 0.626.$$

Physical interpretation

- Some clusters have very large RGB mass losses.
- Axion cooling increases the TRGB luminosity.
- Higher luminosity strengthens Reimers mass loss.
- In extreme cases, this mass loss starts to reduce the final helium-core mass.

Transition regime

For NGC6366, the increase of luminosity due to axion cooling is partly compensated by enhanced mass loss. This produces a transition-like regime close to the hot-flasher evolutionary channel.

Key point

The response of L_{TRGB} to additional cooling is no longer purely monotonic in the usual RGB sense, because

TRGB Luminosity: MESA vs Observational Data (preliminary)

Cluster	$\log L_{\mathrm{MESA}}$	$\log L_{\mathrm{obs}}$	Cluster	$\log L_{\mathrm{MESA}}$	$\log L_{\mathrm{obs}}$
NGC6205	$3.3442^{+0.0201}_{-0.0201}$	$3.0480^{+0.0497}_{-0.0580}$	NGC5904	$3.3732^{+0.0201}_{-0.0201}$	$3.2428^{+0.0334}_{-0.0345}$
NGC6218	$3.3723^{+0.0201}_{-0.0201}$	$3.3112^{+0.0505}_{-0.0625}$	NGC6341	$3.2993^{+0.0201}_{-0.0201}$	$3.2110^{+0.0268}_{-0.0346}$
NGC6093	$3.3440^{+0.0201}_{-0.0201}$	$3.3398^{+0.0608}_{-0.0829}$	NGC0362	$3.3782^{+0.0201}_{-0.0201}$	$3.3729^{+0.0608}_{-0.0838}$
NGC0288	$3.3729^{+0.0201}_{-0.0201}$	$3.0340^{+0.0518}_{-0.0770}$	NGC5053	$3.3058^{+0.0202}_{-0.0202}$	$2.9301^{+0.0850}_{-0.1172}$
NGC6171	$3.3896^{+0.0201}_{-0.0201}$	$3.1671^{+0.0938}_{-0.1441}$	NGC5466	$3.3230^{+0.0201}_{-0.0201}$	$3.2373^{+0.0513}_{-0.1136}$
NGC6352	$3.4002^{+0.0206}_{-0.0206}$	$3.1763^{+0.1044}_{-0.1453}$	NGC6779	$3.3212^{+0.0201}_{-0.0201}$	$3.3609^{+0.0656}_{-0.0847}$
NGC6838	$3.4143^{+0.0201}_{-0.0201}$	$3.3117^{+0.1303}_{-0.3150}$	NGC6101	$3.3247^{+0.0202}_{-0.0202}$	$3.3692^{+0.0943}_{-0.1763}$
NGC7099	$3.3145^{+0.0201}_{-0.0201}$	$3.3788^{+0.0764}_{-0.1442}$	NGC1261	$3.3714^{+0.0202}_{-0.0202}$	$3.3284^{+0.0642}_{-0.0870}$
NGC6723	$3.3917^{+0.0201}_{-0.0201}$	$3.1590^{+0.0967}_{-0.1092}$	NGC6752	$3.3517^{+0.0206}_{-0.0206}$	$3.3248^{+0.0558}_{-0.0700}$
NGC6362	$3.3934^{+0.0201}_{-0.0201}$	$3.2630^{+0.0463}_{-0.0639}$	NGC6809	$3.3269^{+0.0201}_{-0.0201}$	$3.2774^{+0.0330}_{-0.0513}$
NGC5897	$3.3285^{+0.0201}_{-0.0201}$	$3.4835^{+0.1256}_{-0.1921}$	NGC6541	$3.3322^{+0.0201}_{-0.0201}$	$3.2910^{+0.0364}_{-0.0450}$
NGC6366	$3.4047^{+0.0206}_{-0.0206}$	$3.0813^{+0.0648}_{-0.1226}$	NGC6254	$3.3491^{+0.0202}_{-0.0202}$	$3.3111^{+0.0558}_{-0.0955}$
NGC5024	$3.3302^{+0.0201}_{-0.0201}$	$3.2616^{+0.0272}_{-0.0322}$	NGC6397	$3.3290^{+0.0202}_{-0.0202}$	$3.2897^{+0.0521}_{-0.0860}$
NGC5272	$3.3513^{+0.0201}_{-0.0201}$	$3.3145^{+0.0440}_{-0.0489}$			

Conclusions

Main results

- We computed the TRGB luminosities and other stellar parameters for 27 globular clusters using MESA.
- For each cluster, we constructed a grid of models with different values of the axion–electron coupling.
- The results are consistent with the theoretical picture: stronger axion cooling increases the helium-core mass at ignition and makes the TRGB brighter.
- By comparing observations with MESA grids, we obtain a preliminary statistical bound:

$$g_{13} < 0.26$$

- This preliminary result provides the strongest astrophysical constraint on g_{13} in the considered method. Some details will be discussed in the next talk.

Main mechanism

$$g_{13} \uparrow$$
$$\Downarrow$$
$$\epsilon_a \uparrow$$
$$\Downarrow$$
additional core cooling
$$\Downarrow$$
$$M_{\mathrm{He,TRGB}} \uparrow$$
$$\Downarrow$$
$$L_{\mathrm{TRGB}} \uparrow$$

Thank you for your attention

Questions are welcome

Acknowledgements

This work was supported by the Ministry of Science and Higher Education of the Russian Federation, contract No. 075-15-2024-541.